Design and simulation of graphene majority gate without back-gating

Design and Simulation of Graphene Majority Gate without Back-gating

Savvas Moysidis[1], Ioannis G. Karafyllidis[1,*], Panagiotis Dimitrakis[2]

1. Department of Electrical and Computer Engineering, Democritus University of Thrace, 67100 Kimmeria, Xanthi, Greece
2. Institute of Nanoscience and Nanotechnology, NCSR "Demokritos", 15 310 Aghia Paraskevi, Athens, Greece
* Author to whom any correspondence should be addressed (e-mail: ykar@ee.duth.gr).

Abstract

Graphene is a two-dimensional carbon allotrope with excellent biocompatibility allowing for safe integration in living tissue and is stable in harsh biological environments. Graphene has also very high electron mobilities and long carrier mean-free paths and is a very promising material for new nanoelectronic circuits. Here we present the design and simulation of a graphene Majority logic gate without back-gating, which can be fabricated on one side of the graphene sheet leaving the other free so that the gate can be brought into contact with biological tissue. Graphene majority gates can also operate as AND or OR gates giving rise to new carbon-based nanoelectronic devices for biomedical circuits.

Keywords: Nanoelectronics, Graphene Logic Gates, Non-equilibrium Green function, Design, Simulation.

1. Introduction

G RAPHENE is a promising new material for bioelectronic and biomedical applications [1,2]. Graphene is flexible, biocompatible, chemically stable, and has low intrinsic electronic noise, properties that have been exploited for the fabrication of solution-gated field-effect transistors used to monitor neural cells and brain activity [3,4]. Furthermore, graphene's mechanical properties combined with its high thermal and electrical conductivities make graphene a very useful scaffolding material that can also promote tissue regeneration [5]. On the other hand, graphene is a promising material for high-speed, low-power circuits because of its excellent electronic properties [6,7].

It would be highly desirable to be able to fabricate graphene logic nanoelectronic circuits that would be incorporated in living tissue to perform computations locally. This would provide new possibilities for monitoring and controlling biochemical processes that include ion transport. The absence of a bandgap in graphene results in poor conductance modulation which is a considerable obstacle for the development of such logic circuits [7,8]. Recently, it has been shown that effective conductance modulation is possible in specific graphene nanoribbon geometries, especially quantum point contacts and L-shaped and T-shaped

graphene nanoribbons when combined with potentials applied through top and back-gates [9-15]. Here we use the conclusions on the effect of L and T graphene nanoribbon shapes on conductance, studied in [12], to design the majority gates. L and T shaped nanoribbons are used as structural elements of the majority gate.

A graphene logic gate for biological applications should be universal, with no back-gates, allowing one of the graphene sheet sides to be brought into contact with biological systems, such as living tissue or cell cultivations [5]. Here we present the design and simulation of such a logic gate. We design a graphene Majority logic gate, which can also operate as an OR or a NOT gate providing Boolean universality. This logic gate does not require back-gating and the effective conductance modulation is obtained by combining L-shaped and T-shaped graphene nanoribbons in which potentials are only applied through top-gates. We use tight-bind Hamiltonians and the non-equilibrium Green function method (NEGF) to compute the conductance of the Majority gate for various applied input potentials and show that the majority gate truth table is executed exactly using only two potential values representing the logic zero and one.

This paper is organized as follows: In section two we briefly describe the NEGF method, in section three we present the geometry and the Majority gate inputs and output, in section four we present the computation of the Majority gate conductance for all possible input values and show that the truth table is followed exactly. We discuss our results in section five.

2. The NEGF method for carrier transport

NEGF is a quantum mechanical method with very high predictive power, the results of which are very close or even identical to experimental results [19-21]. The nanoconductor, the conductance of which is to be computed is described by a tight-binding Hamiltonian matrix, H, which describes the kinetic and potential energy of electrons. The potential energy enters through the diagonal elements and the kinetic energy through the off-diagonal elements of H, assuming electron hoping between nearest-neighboring atoms only [22-24]. The Hamiltonian fully describes the isolated nanoconductor and the effect of the contacts is described by the contact self-energies, Σ. The retarded Green's function, G^R, and the advanced Green's function, G^A, are propagators describing the amplitudes of electron transport form one contact to another contact through the nanoconductor:

$$G^R = \left[\left(E + i\,\eta^+ \right) I - H - \sum_{k=1}^{n} \Sigma_k \right]^{-1}$$ (1)

$$G^A = \left(G^R \right)^+$$ (2)

E is the energy of transported electrons, I the unit matrix, η^+ is a very small energy value multiplied by the imaginary unit i, and Σ are the self-energies of the contacts, the number of which in the case of eq. (1) is n. Each contact is related to a broadening function, Γ:

$$\Gamma_k = i\left[\Sigma_k - \Sigma_k^+ \right]$$ (3)

The potential difference between any two contacts l and m enters through the Fermi functions, f, of these contacts:

$$\Sigma^{in} = f_l\,\Gamma_l + f_m\,\Gamma_m$$ (4)

The electron density G^n is computed from:

$$G^n = G^R \, \Sigma^{in} \, G^A \tag{5}$$

The density of states is:

$$A = i \left(G^R - G^A \right) \tag{6}$$

The conductance, $G_{l,m}(E)$, between any two contacts l and m depends on the electron energy, E, and is given by:

$$G_{l,m}(E) = \frac{2\,q^2}{h} Trace\left[\, \Gamma_l \, G^R \, \Gamma_m \, G^A \, \right] \tag{7}$$

Once the conductance is computed, the current flowing between any two contacts is computed using Landauer's formula:

$$I_{l,m} = \frac{q}{h} \int_{-\infty}^{\infty} \left(f_l(E) - f_m(E) \right) \frac{G_{l,m}(E)}{q^2 / h} \, dE \tag{8}$$

Biological processes involving ion transport, or ion density variations through the activation of ion channels, alter the conductance of the graphene nanoribbons and result in recordable current variations. Control of ion motion can be obtained by proper current variation. Current variation is a result of the modulation of conductance given by equation (7). As we will describe in the sections to follow, conductance can be effectively modulated in the Majority graphene gate by constructing it using L and T-shaped nanoribbons and by applying top-gate potentials.

3. Structure of the graphene majority gate

The circuit symbol of the majority gate, M, is shown in Fig. 1. The gate has three inputs, A, B and C and one output, OUT. The gate output takes the value of the majority of inputs, as shown by the gate truth table, Table I.
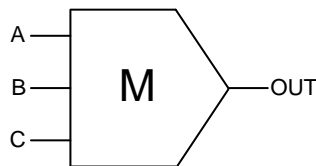
Fig. 1. The circuit symbol of the majority gate, M.

TABLE I
MAJORITY GATE TRUTH TABLE

A	B	C	OUT
0	0	0	0
0	0	1	0
0	1	0	0
0	1	1	1
1	0	0	0
1	0	1	1
1	1	0	1
1	1	1	1

Fig. 2. Up: Top view of the graphene Majority gate. Down: Cross section of the graphene Majority gate along the (red) PQ dashed line.

Figure 2 shows the structure of the graphene Majority gate. The upper part of Fig. 2 shows the top view of the gate and the lower part shows a cross section along the (red) PQ dashed line. The graphene

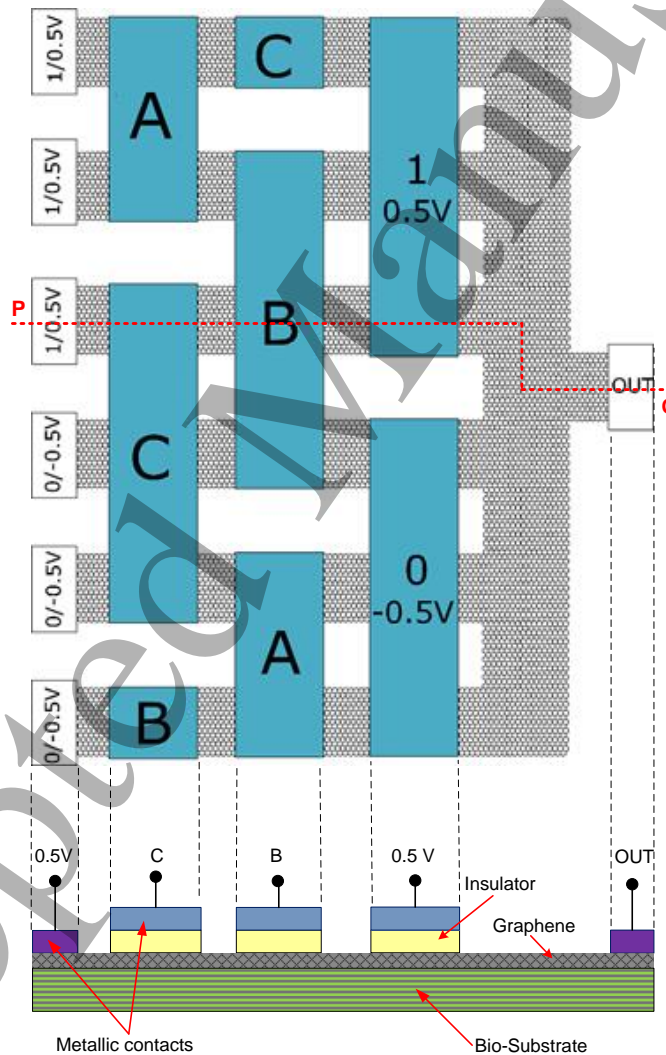Majority gate comprises six horizontal and one vertical graphene nanoribbon forming L and T shapes. There is also a small horizontal nanoribbon connecting the output, OUT, electrode with the vertical nanoribbon. All horizontal graphene nanoribbon edges are zig-zag edges and all vertical graphene nanoribbon edges are armchair edges. As shown in [12] this change in electron transport direction, from zig-zag edged graphene, which is metallic to armchair edged graphene, which is semiconducting gives rise to a pseudo-bandgap which, along with the applied potentials, results is effective conductance modulation.

The logical "1" is represented by a potential equal to 0.5 V and the logical "0" by a potential equal to -0.5V. These two potential values are the only potential values used to operate the gate. The three upper horizontal nanoribbons are connected to constant potentials equal to 0.5 V representing the logical "1". These contacts are indicated in Fig. 2 by "1/0.5V". The three lower nanoribbons are also connected to constant potentials equal to -0.5 V representing the logical "0". These contacts are indicated in Fig. 2 by "0/-0.5V". These conducts, and the output contact, OUT, are metallic electrodes connected directly to the graphene nanoribbons, allowing electron transport through them.

A constant common top-gate potential equal to 0.5 V is applied to the three upper horizontal graphene nanoribbons. This potential is applied through an insulating layer and affects the energies of the transported electrons, but no electrons can be induced or extracted through these top-gates due to the insulating layer. This common top-gate electrode is indicated by "1/0.5 V" in Fig. 2. A constant common top-gate potential equal to -0.5 V is also applied to the three lower horizontal graphene nanoribbons. This common top-gate electrode is indicated by "0/-0.5 V" in Fig. 2. Since this potential is also applied through an insulating layer it affects the transported electron energy, but no electrons can be induced or extracted through these top-gates. The constant potentials applied through direct contacts or top-gates correspond to the V_{DD} and V_{SS} potentials used in microelectronic logic gates.

The three Majority gate inputs A, B and C are applied through top-gates, separated from the graphene sheet by an insulating material. Each input is applied through top-gates indicated by A, B and C in Fig. 2. The input potentials can only take values equal to 0.5 V or "1", and equal to -0.5 V or "0". Each one of the eight possible input potential combinations correspond to a truth table line. The output potential, OUT, can take only two values, -0.5 V or 0.5 V, corresponding to "0" and "1".

All electrodes are placed on the one side of the graphene sheet allowing the other one to be brought into contact with bio-substrates, such as tissues of cell cultivations. Graphene is a very dense material and does not allow the transport of atoms or molecules, such as used to form the metallic contacts and the insulating layers, through it [7]. This property ensures that the bio-substrate will not be contaminated by these atoms or molecules.

4. Operation of the graphene majority gate

The operation of the Majority graphene gate is simulated using tight-binding Hamiltonians combined with the NEGF method. We compute the conductance of each one of the horizontal graphene nanoribbons of the structure shown in Fig. 2 for the eight possible input potentials applied through electrodes A, B and C. The horizontal nanoribbons are numbered from 1 to 6, from top to bottom of Fig. 2. Figure 3 shows the conductance of each one of the six horizontal nanoribbons when the input potentials A, B and C are all equal to -0.5 V, which corresponds to the first line of the truth table.
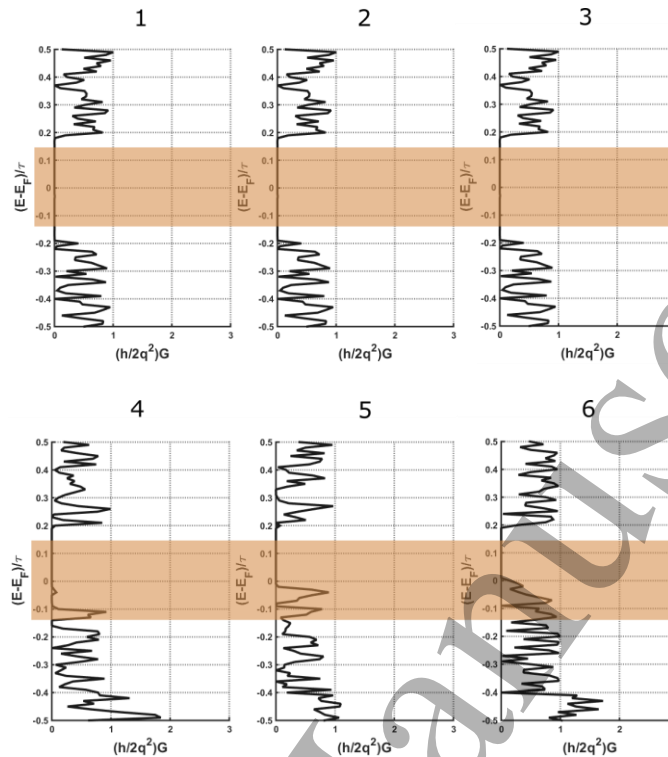
Fig. 3. Computed conductance of the six horizontal nanoribbons of the structure shown in Fig. 2, for input potentials A = B = C= -0.5 V. These input values correspond to the first line of the truth table. The nanoribbons are numbered from top to bottom.

The *y-axes* of all diagrams are the electron energy $(E-E_F)/\tau$, where E_F is the Fermi energy and τ is the overlap integral value corresponding to electron hoping, which has been measured to be equal to *-2.7 eV* in graphene. The *x-axes* give the value of the normalized conductance, $(h/2q^2)G$, as a function of electron energy, computed using eq. (7). Only electrons with energies a few *kT* below and above the Fermi energy participate in the conductance and this energy range is indicated by the orange bands in Figure 3. The conductance of horizontal nanoribbons 1, 2 and 3 is zero in this energy range, and because of eq. (8), no current flows through them. Therefore, none of the three constant potentials (1/0.5 V) is transferred to the output. The conductance of nanoribbons 4, 5 and 6 is nonzero in this energy range, and the constant potentials (0/-0.5 V) are transferred in parallel to the output OUT the potential of which becomes -0.5 V corresponding to logical "0". The first line of the truth table is executed by the graphene Majority gate.
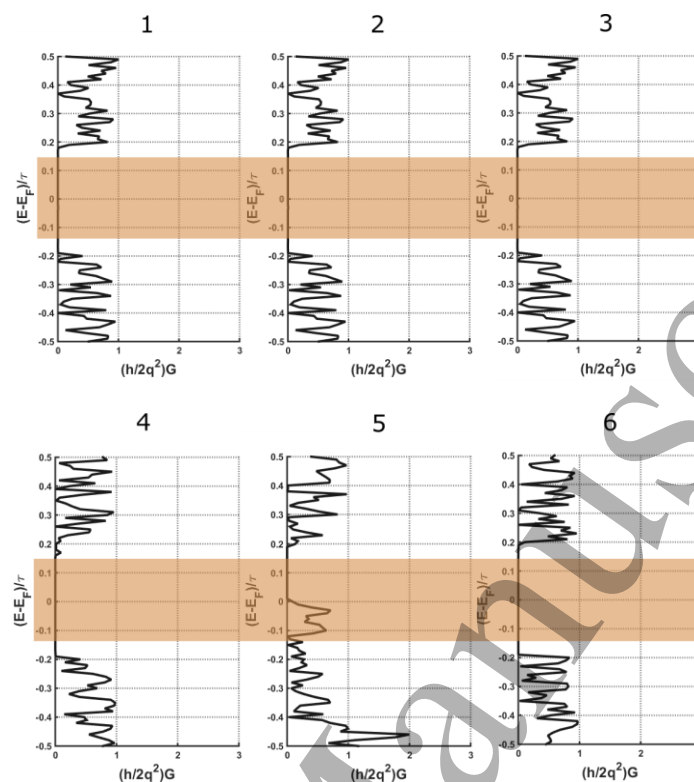
Fig. 4. Computed conductance of the six horizontal nanoribbons of the structure shown in Fig. 2, for input potentials A = B = -0.5 V and C= 0.5 V. These input values correspond to the second line of the truth table.

Figure 4 shows the conductance of each one of the six horizontal nanoribbons when the input potentials A and B are equal to -0.5 V and C equals to 0.5 V, which corresponds to the second line of the truth table. In this case only nanoribbon 5 conducts and the constant potential (0/-0.5 V) is transferred to the output, the potential of which becomes -0.5 V corresponding to logical "0" in compliance with the second line of the truth table.

For the third line of the truth table, the computed conductance of the six horizontal nanoribbons is shown in Fig. 5. In this case the input potentials A and C are equal to -0.5 V and the input potential B is equal to 0.5 V. Only nanoribbon 4 is conducting and the constant potential (0/-0.5 V) is transferred to the output, which in this case corresponds to logical "0".

The execution of the logical operation of the fourth line of the majority gate truth table is shown in Fig. 6. The input potentials B and C are set equal to 0.5 V and the input potential A to -0.5 V. As shown in this figure only nanoribbon 3 conducts for this input potential combination. As a result, the constant potential (1/0.5 V) is transferred to the output setting it at logical "1".

Fig. 5. Computed conductance of the six horizontal nanoribbons of the structure shown in Fig. 2, for input potentials A = C = -0.5 V and B= 0.5 V. These input values correspond to the third line of the truth table.

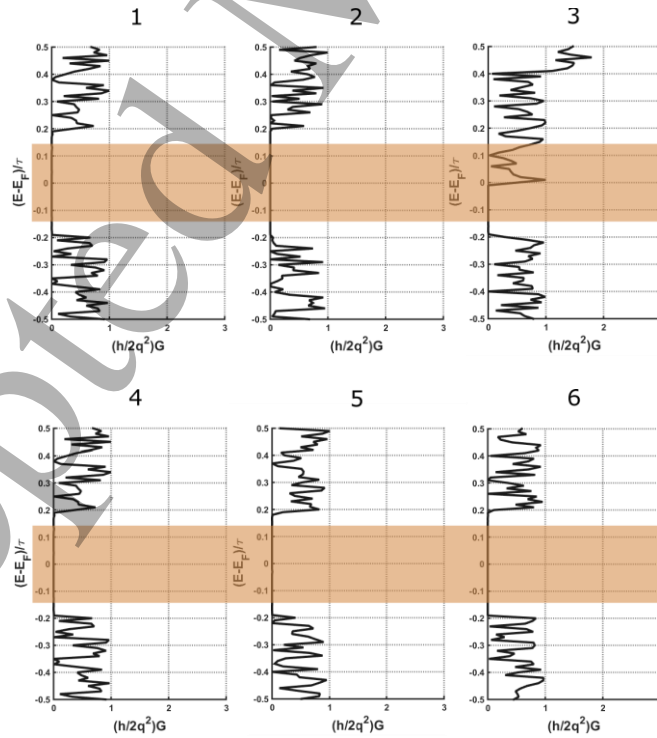Fig. 6. Computed conductance of the six horizontal nanoribbons of the structure shown in Fig. 2, for input potentials A = -0.5 V and B = C = 0.5 V. These input values correspond to the fourth line of the truth table.

Fig. 7 shows the conductance of the six nanoribbons comprising the majority gate, when the input potentials are: A=0.5 V and B = C = -0.5 V. In this case the fifth line of the gate's truth table is executed, because only nanoribbon 6 conducts transferring the constant potential (0/-0.5 V) to the output, setting it to the logical "0".
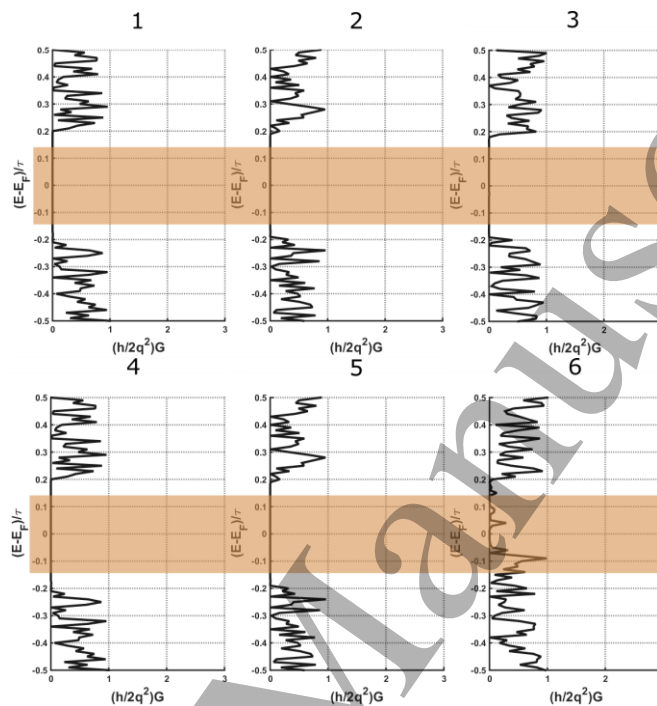

Fig. 7. Computed conductance of the six horizontal nanoribbons of the structure shown in Fig. 2, for input potentials A = 0.5 V and B = C = - 0.5 V. These input values correspond to the fifth line of the truth table.

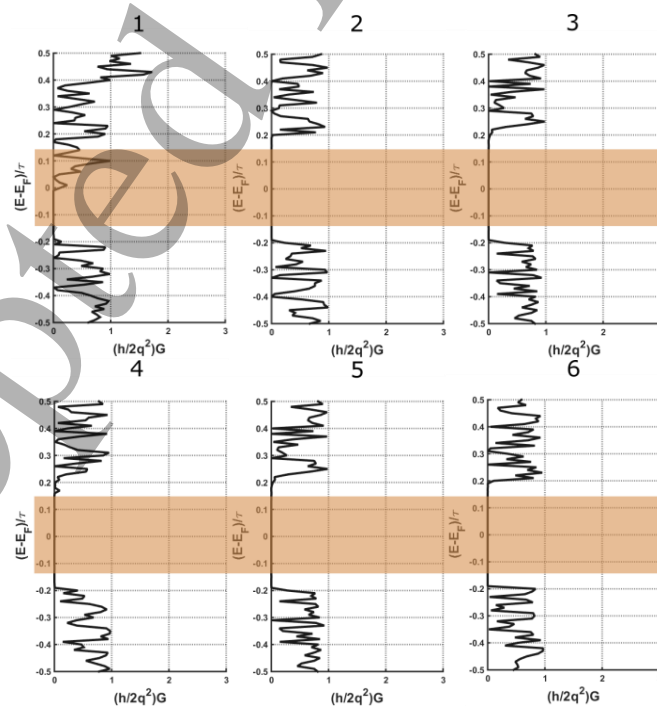
Fig. 8. Computed conductance of the six horizontal nanoribbons of the structure shown in Fig. 2, for input potentials A = C = 0.5 V and B = - 0.5 V. These input values correspond to the sixth line of the truth table.

AUTHOR SUBMITTED MANUSCRIPT - ERX-100107.R2

Page 10 of 13

IOP Publishing

Journal Title

Journal **XX** (XXXX) XXXXXX

https://doi.org/XXXX/XXXX

To execute the sixth line of the truth table the potential of the majority gate inputs A and C is set equal to 0.5 V and the potential of the input B is set equal to -0.5 V. Our computations showed that in this case only nanoribbon 1 is in conductive state and the constant potential (1/0.5 V) is transferred to the output, which is set to logical "1". This case is shown in Fig.8.

Figure 9 shows the conductance of each one of the six horizontal nanoribbons when the input potentials A and B are equal to 0.5 V and C equals to -0.5 V, which corresponds to the seventh line of the truth table. In this case only nanoribbon 2 conducts and the constant potential (1/0.5 V) is transferred to the output, the potential of which becomes 0.5 V corresponding to logical "1" according to the seventh line of the truth table.
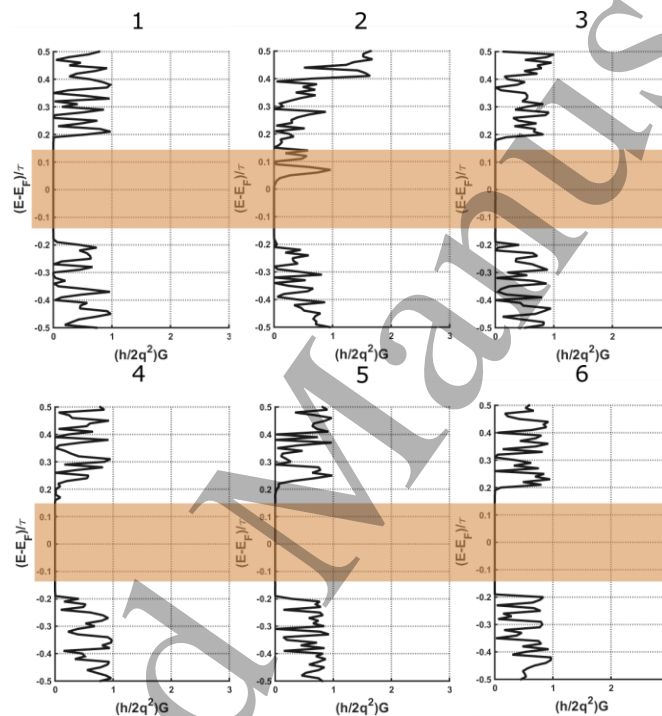

Fig. 9. Computed conductance of the six horizontal nanoribbons of the structure shown in Fig. 2, for input potentials A = B = 0.5 V and C= -0.5 V. These input values correspond to the seventh line of the truth table.

Figure 10 shows the conductance of each one of the six horizontal nanoribbons when the input potentials A, B and C are equal to 0.5 V, which corresponds to the eighth line of the truth table. In this case nanoribbons 4, 5 and 6 do not conduct, whereas nanoribbons 1, 2 and 3 conduct and the constant potentials (1/0.5 V) are transferred in parallel to the output the potential of which becomes equal to 0.5 V corresponding to logical "1" according to the last line of the truth table.

Recapitulating the majority gate operation, in the case of the first line of the truth table only nanoribbons 4, 5 and 6 are in conductive state. In the case of the second line of the truth table, only nanoribbon 5 conducts. Only nanoribbon 4 conducts for the input potential combinations corresponding to the third line of the truth table. For the input potentials combination corresponding to the fourth truth table line, only nanoribbon 3 conducts. In the case of the fifth line of the truth table, only nanoribbon 6 conducts and in the case of the sixth line, only nanoribbon 1 is in conductive state. In the case of the seventh truth table line, only nanoribbon 2 is conducting and in the case of the eight line only nanoribbons 1, 2 and 3 conduct.
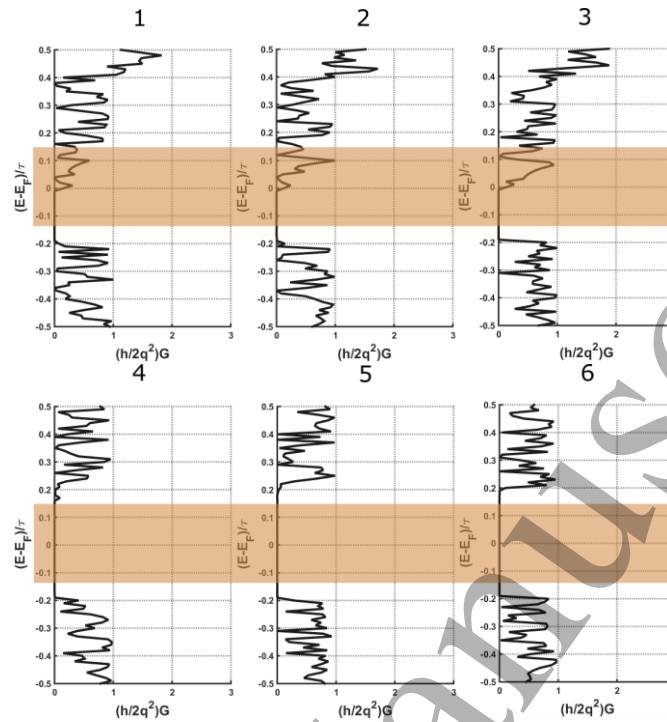
Fig. 10. Computed conductance of the six horizontal nanoribbons of the structure shown in Fig. 2, for input potentials A = B = C = 0.5 V. These input values correspond to the last line of the truth table.

TABLE II
CONDUCTIVE, "C", AND NON-CONDUCTIVE, "N", STATES OF THE SIX HORIZONTAL MAJORITY GATE NANORIBBONS. TABLE ROWS CORRESPOND TO THE TRUTH TABLE LINES

1	2	3	4	5	6
N	N	N	**C**	**C**	**C**
N	N	N	N	**C**	N
N	N	N	**C**	N	N
N	N	**C**	N	N	N
N	N	N	N	N	**C**
C	N	N	N	N	N
N	**C**	N	N	N	N
C	**C**	**C**	N	N	N

Table II shows the state of conductance of the six horizontal nanoribbons for all eight input potential combinations of the majority gate truth table. Each row of Table II corresponds to one row of the truth table. The columns of Table II correspond to the six horizontal nanoribbons. The letter "C" indicates that the nanoribbon is conductive and the letter "N" that the nanoribbon is in non-conductive state.

5. Conclusion

We presented the design and simulation of a Majority graphene gate, using tight-binding Hamiltonians and the NEGF method. The structure of the gate combined with applied top-gate potentials results in effective conductance modulation and accurate execution of the Majority gate truth table without using

back-gates. The lack of back-gates leaves one of the graphene sheet sides free to be incorporated with biological substrates. The universality of the Majority gate and the density of the graphene sheet combined with its biocompatibility hold great promise for the development of graphene circuits for biological and biomedical applications.

Acknowledgements

References

[1] Amel Bendali, Lucas H. Hess, Max Seifert, Valerie Forster, Anne-Fleur Stephan, Jose A. Garrido and Serge Picaud, "Purified Neurons can Survive on Peptide-Free Graphene Layers", *Advanced Healthcare Materials*, vol. 2, pp. 929-933, 2013.

[2] Yasuhide Ohno, Kenzo Maehashi, Yusuke Yamashiro, and Kazuhiko Matsumoto, "Electrolyte-Gated Graphene Field-Effect Transistors for Detecting pH and Protein Adsorption", *Nano Letters,* vol. 9, pp. 3318-3322, 2009.

[3] Benno M Blaschke, Núria Tort-Colet, Anton Guimerà-Brunet, Julia Weinert, and Lionel Rousseau, "Mapping brain activity with flexible graphene micro-transistors", *2D Materials,* vol. 4, 025040, 2017.

[4] Ji Cheng, Lei Wu, Xiao-Wei Du, Qing-Hui Jin, Jian-Long Zhao and Yuan-Sen Xu, "Flexible Solution-Gated Graphene Field Effect Transistor for Electrophysiological Recording", *Journal of Microelectromechanical Systems*, vol. 23, pp. 1311 - 1317, 2014.

[5] Xiaowei Wu, Shinn-Jyh Ding, Kaili Lin, and Jiansheng Su, "A review on the biocompatibility and potential applications of graphene in inducing cell differentiation and tissue regeneration", *Journal of Material Chemistry B*, vol. 5, pp. 3084-3102, 2017.

[6] A. H. Castro Neto, F. Guinea, N. M. R. Peres, K. S. Novoselov and A. K. Geim, "The electronic properties of graphene", *Reviews of Modern Physics*, vol. 81, pp. 109-162, 2009.

[7] E. L. Wolf, *Graphene*, Oxford University Press, Oxford, UK, 2014.

[8] Frank Schwierz, "Graphene transistors", Nature Nanotechnology, vol. 5, pp. 487-496, 2010.

[9] T. Low, S. Hong, J. Appenzeller, S. Datta and M. S. Lundstrom, "Conductance Asymmetry of Graphene p-n Junctions" IEEE Transactions on Electron Devices, vol. 56, pp.1292-1299, 2009.

[10] I. G. Karafyllidis, "Current Switching in Graphene Quantum Point Contacts", *IEEE Transactions on Nanotechnology*, vol. 13, pp. 820-814, e2014.

[11] B. Huard, J. A. Sulpizio, N. Stander, K. Todd, B. Yang, and D. Goldhaber-Gordon, "Transport Measurements Across a Tunable Potential Barrier in Graphene", *Physical Review Letters*, vol. 98, 236803, 2007.

[12] S. Moysidis and I. G. Karafyllidis, "Conductance of L-shaped and T-shaped graphene nanoribbons", *Microelectronics Journal*, vol. 72, pp. 11-13, 2018

[13] I. Nikiforidis, I. G. Karafyllidis and P. Dimitrakis, "Simulation and parametric analysis of graphene p-n junctions with two rectangular top-gates and a single back gate", *Journal of Physics D: Applied Physics*, vol. 51, 075303, 2018.

[14] S. Moysidis, I. G. Karafyllidis, and P. Dimitrakis, "Graphene logic gates", *IEEE Transactions on Nanotechnology*, vol. 17, pp. 852 – 859, 2018.

[15] Hsin-Ying Chiu, V. Perebeinos, Yu-Ming Lin, and Ph. Avouris, "Controllable p-n Junction Formation in Monolayer Graphene Using Electrostatic Substrate Engineering", Nano Letters, vol. 10, pp. 4634-4639, 2010.

[16] Y. Jiang, N. C. Laurenciu, He Wang and S. D. Cotofana, "Graphene Nanoribbon Based Complementary Logic Gates and Circuits", IEEE Transactions on Nanotechnology, vol. 18, pp. 287 – 298, 2019.

[17] Y. Jiang, N. C. Laurenciu,and S. D. Cotofana, "On Basic Boolean Function Graphene Nanoribbon Conductance Mapping", IEEE Transactions on Circuits and Systems I, vol. 66, pp 1948 - 1959, 2019.

[18] Y. Jiang, N. C Laurenciu,and S. D. Cotofana, "On Carving Basic Boolean Functions on Graphene Nanoribbons Conduction Maps", 2018 IEEE International Symposium on Circuits and Systems (ISCAS), Florence, Italy, 2018.

[19] Supriyo Datta, *Lessons from Nanoelectronics – A new perspective on transport,* World Scientific, London, 2012.

[20] S. Datta, "Nanoscale device modeling: the Green's function method", *Superlattices and Microstructures*, vol. 28, pp. 253-278, 2000.

[21] G. Rickayzen, *Green's Functions and Condensed Matter*, Dover Publications, London, 2013

[22] C. Bena and G. Montambaux, "Remarks on the tight-binding model of graphene", *New Journal of Physics*, vol. 11, 095003, 2009.

[23] S. Reich, J. Maultzsch, C. Thomsen and P. Odréjon, "Tight-binding description of graphene*", Physical Review B*, vol. 66, 035412, 2002.

[24] S. Datta, "Nanoscale device modeling: the Green's function method", *Superlattices and Microstructures*, vol. 28, pp. 253-278, 2000.